DNA INTERACTION AND CYTOTOXICITY OF THE PLATINUM BLUE COMPLEX CONTAINING 2-AMINOTHIOPHENOL

A MASTER'S THESIS

in

Chemical Engineering and Applied Chemistry

Atilim University

by

SAFIA SALEM

January 2017

DNA INTERACTION AND CYTOTOXICITY OF THE PLATINUM BLUE COMPLEX CONTAINING 2-AMINOTHIOPHENOL

A THESIS SUBMITTED TO

THE GRADUATE SCHOOL OF NATURAL AND APPLIED SCIENCES

OF

ATILIM UNIVERSITY

BY

SAFIA SALEM

IN PARTIAL FULFILLMENT OF THE REQUIREMENTS FOR THE DEGREE OF MASTER OF SCIENCE

IN

APPLIED CHEMISTRY

AT

THE DEPARTMENT OF CHEMCAL ENGINEERING AND APPLIED CHEMISTRY

January 2017

Approval of the Graduate School of Natural and Applied Sciences, Atılım University.

_____

Prof. Dr. İbrahim Akman

I certify that this thesis satisfies all the requirements as a thesis for the degree of Master of Science.

_____

Prof. Dr. Atilla Cihaner

Head of Department

This is to certify that we have read the thesis "DNA Interaction and Cytotoxicity of the Platinum Blue Complex Containing 2-aminothiophenol" submitted by "SAFIA SALEM" and that in our opinion it is fully adequate, in scope and quality, as a thesis for the degree of Master of Science.

_____

Prof. Dr. Şeniz Özalp Yaman

Supervisor

Examining Committee Members

Prof. Dr. Şeniz Özalp Yaman _____

Prof. Dr. Nezire Saygılı _____

Assist. Prof. Dr. Hakan Kayı _____

Date: 26.01.2017

I declare and guarantee that all data, knowledge and information in this document has been obtained, processed and presented in accordance with academic rules and ethical conduct. Based on these rules and conduct, I have fully cited and referenced all material and results that are not original to this work.

Name, Last name: SAFIA SALEM

Signature:

ABSTRACT

DNA INTERACTION AND CYTOTOXICITY OF THE PLATINUM BLUE COMPLEX CONTAINING 2-AMINOTHIOPHENOL

SAFIA SALEM

Supervisor: Prof. Dr. Şeniz ÖZALP YAMAN

2017, 47 pages

Since the discovery of cisplatin, metal based agents have gained significant interest of researchers as potential anticancer drugs. Several drugs have been rationally synthesized to overcome the hurdles of cisplatin, majorly its toxicity and resistance. Search for less toxic, but still potent anti-cancer platinum compounds revealed a class of platinum complexes with pyrimidines called platinum-pyrimidine complexes also known as "platinum blue" (Pt-blue) complexes. Here, we describe DNA binding ability of the Pt-blue complex $[Pt_4(2\text{-atp})_8(H_2O)(OH)]$ (2-atp: 2- aminothiophenol).

In order to investigate the nature of the interaction between the Pt-blue complex and DNA, spectroscopic measurements were made and the results of UV titration, thermal behavior, viscosity and fluorometric titration of the Pt-blue treated DNA were evaluated. Our results suggested that the compound was able to partially intercalate DNA that related to the anticancer activities of the drugs.

Keywords: Antitumor drugs, platinum blue complexes, DNA binding ability, cytotoxicity.

ÖZ

2-AMİNOTİYOFENOL İÇEREN PLATİN MAVİSİ KOMPLEKSİNİN DNA ETKİLEŞİMİ VE SİTOTOKSİSİTESİ

SAFIA SALEM

Tez Yöneticisi:Prof. Dr. Şeniz ÖZALP YAMAN

2017, 46 pages

Cis platinin keşfinden bu yana, metal içeren ajanlar potansiyel birer antikanser ilacı olarak araştırmacıların ilgisini çekmektedir. Bu güne kadar cis platinin toksik etkilerini ve cis platin direncini azaltmak için birçok ilaç sentezlenmiştir. Bu bileşiklerden bir tanesi de "platin mavisi" olarak bilinen, toksisitesi cis platine göre daha düşük ve antikanser özelliği yüksek olan farklı bir platin kompleksi sınıfıdır. Bu çalışmada, $[Pt_4(2\text{-atp})_8(H_2O)(OH)]$ (2-atp: 2- aminotiyofenol) formülüyle gösterilen yeni platin mavisi kompleksinin DNA'ya bağlanma kabiliyeti araştırılmıştır.

Pt mavisi ve DNA arasındaki etkileşim türünün belirlenebilmesi için spektroskopik ölçümler yapılmış, platin kompleksinin varlığında DNA çözeltisinin UV-titrasyon, termal bozunma, viskozite değişim ve florometrik titrasyon deneyleri tamamlanmıştır. Sonuçlar platin mavisi bileşiğinin DNA'ya kısmen interkaltif olarak bağlandığını ve antikanser özelliği gösterdiğini kanıtlamıştır.

Anahtar Kelimeler: Antitumör ilaçlar, platin mavisi kompleksleri, DNA bağlanma kabiliyeti, sitotoksisite

To My Parents

ACKNOWLEDGMENTS

I express sincere appreciation to my supervisor Prof. Dr. Şeniz Özalp Yaman for her guidance and insight throughout the project.

Acknowledge to Assoc. Prof. Dr. Ceyda Açılan Ayhan for performing cytotoxicity experiments in TÜBİTAK Marmara Research Center.

I want to thank to Libyan government and Libyan Embassy for their valuable financial support during my studies in Atılım University.

Thank to my family and friends for their support, trust and encouragement.

I am grateful to my husband, Mohamed for his continuous support and patience during this period.

I would also like to express my thanks to all stuff in Atılım University, Chemical Engineering and Applied Chemistry Department for their support during this study.

This work is supported by the grants ATU-BAP/2006/04 provided by Atılım University and internal funding by TUBITAK, Marmara Research Center.

TABLE OF CONTENTS

LIST OF FIGURES

LIST OF TABLE

CHAPTER 1

INTRODUCTION

1.1. Platinum Complexes

Coordination complexes have been known since the beginning of modern chemistry. One of the well-known coordination complexes is Prussian blue and their properties were well understood in the late 1800s, following the work of Christian Wilhelm Blomstrand who is the father of "the complex ion chain theory". Blomstrand indicated that the reason of the formation of the coordination compounds was the interaction of the ions in the solutions with the ammonia chains. Afterwards, he repeated the same reactions by changing the ammonia chains with the various carbohydrate chains. Following this theory, Danish scientist Jorgensen investigated the possible outcomes of the reactions in the solutions containing metals. According to the proposed mechanism, ions would either bind via ammonia chains as the Blomstrand claimed or the ions would bind directly to the metal [1].

The most widely accepted version of the coordination complex theory was published by Alfred Werner, in 1914. Werner described two different ion locations in the coordination complexes; the inner sphere (coordination sphere) and/or the outer

sphere [2]. Werner discovered the spatial arrangement of the ligands when they coordinated to the cobalt while indicating the importance of the charge balancing in the coordination complexes.

Platinum and platinum based coordination compounds, on the other hand, take the interest of the scientist not only for its industrial usage but also for their unusual colors. Platinum was officially discovered in 1735 in South America. However, the metal was first discovered and used by pre-Columbian Indians. The name originates from the Spanish word "platina" meaning "silver". Platinum is used in the chemicals industry as a catalyst. It is also used as a catalyst to improve the efficiency of fuel cells. Platinum is important in electronics industry for the production of computer hard disks and thermocouples. Platinum is also used to make optical fibers and LCDs, turbine blades, spark plugs, pacemakers and dental fillings [3].

White organic light-emitting diodes (WOLEDs) have vital attention due to their potential applications in full-panel displays and solid- state lighting. Generally, two or three emitters are needed in a device's configuration to get white light emission. In order to realize high quality (high color rendering index, CRI) and high electroluminescence (EL) efficiency WOLEDs, three phosphorescent dopants (red, green and blue) are used. Fabrication of WOLEDs, on the other hand, is very difficult and blue phosphorescent dopants still unstable [4]. To achieve stable WOLEDs and have an easy fabrication, fluorescent (F)- phosphorescent (P) hybrid WOLEDs have been demonstrated before [5] . Many reports indicated that iridium complexes are very suitable for the production of such F-P hybrid WOLEDs and most of them have high EL efficiency [6]. On the Other hand, platinum complexes have the high quality of F-P hybrid more than iridium complexes due to their square planar geometry and prone to aggregation in the solid state. Platinum complexes often display broadened EL spectra because of its monomeric and eximeric emission. For that reasons, WOLEDs can be easily produced with high quality when combined with blue fluorescent host material such as a high performance *N,N′* –di-1-naphthalenyl-*N,N′*-diphenyl-[1,1′ :4′, 1″:4",1‴ -quaterphenyl]- 4,4‴ –diamine (4P-NPD) [7].

More recently, synthesis and characterization as well as electrochemical, photophysical properties, and X-ray crystallographic studies of four heteroleptic platinum complexes bearing 4-hydroxy-1,5-naphthyridine derivatives functionalized with dimethyl, phenoxy, piperidine or carbazole units were reported by Poloek et al. to achieve hybrid WOLEDs in order to tuning emission energy in solution and in the solid state [6]. The results showed that all of platinum complexes exhibit a wide emission spectrum from greenish yellow in CBP (4,4′-di(9h-carbazol-9-yl)1-1′-biphenyl) hosted thin film to red wavelengths in the 4P-NPD (*N,N′* –di-1-naphthalenyl-*N,N′*-diphenyl-[1,1′ :4′, 1″:4",1‴ -quaterphenyl]- 4,4‴ –diamine). The results also clearly demonstrate the good potential of hybrid WOLEDs having a double emitting layer (CBP) and (4P-NPD) design together with a high blue fluorescent host and dual phosphorescent from a single platinum complex dopant for display and lighting applications [6].

One year later, the same group was able to separately control the emission of the monomer and excimeric\aggregate forms by doping the platinum complex in the CBP and 4P-NDP host materials, respectively. Unlike previously reported hybrid WOLEDs based on single platinum complex dopants, newly generated WOLEDs exhibit little variation in CIE*x,y (*white color chromaticity*)* and the CRI (high color rendering index) for a device driving voltage between 7-10 V. Despite this beneficial feature for WOLED lighting applications, but during this study, the group have found a compromising result between CIE*x,y* and EL (Electro Luminescence) efficiency [8].

The square planar cyclometalated Pt(II) complexes have the specificity of the electronic structure which allows the adduct of binuclear complexes with metal- metal bond luminescing in the red spectral region, that determined the possibility of using the light – emitting diodes and the sensitivity of their optical properties to vapors of organic materials [9].

The spectral and luminescent properties of binuclear cyclometalated Pd(II) complexes are reported in much less than of Pt(II) complexes [10]. Balashev et al. studied the comparison of the optical and electrochemical properties of $[M(C\hat{}N)(\mu\text{-}(N\text{-}S)]_2$ complexes (M=Pd(II), Pt(II); $(C\hat{}N)^-$ are the deprotonated forms of 2-tolylpyridine and benzo[h]quinoline ; $(N\text{-}S)^-$ are pyridine -2-thiolate and benzothiazole -

2- tiolate ions, and the results showed that Pt(II) complexes in each frozen (77K) and liquid (293K) solution end up with luminescence in the red spectral region but for the Pd(II) complexes the luminescence in liquid solution is quenched and their luminescence observed in the red region only below photo excitation of their frozen solution [11].

The effect of the nature of the platinated and bridging mercapto ligands on the electrochemical and optical properties of $[Pt(C\hat{}N)(\mu\text{-}(N\text{-}S))]_2$ complexes as compared with $[Pt(C\hat{}N)En]\ PF_6$ complexes (En is ethylenediamine) were also studied by Balashev et al .The results indicated that the luminescence of binuclear complexes in solution is attributed to the spin- forbidden metal-metal-to-ligand charge transfer (MMLCT) optical transition at the room temperature. In addition, this spin –forbidden radiative processes take place from the intraligand ($\pi_{(C\hat{}N)}$ - $\pi^*_{(C\hat{}N)}$) and meal- to- ligand charge transfer (d_{pt}- $\pi^*_{(C\hat{}N)}$) excited states [12].

In another study, the X-ray diffraction, ^{1}H-NMR and the electronic absorption spectroscopy of binuclear cyclometalated Pt(II) with 2-phenylbenzothiazole and pyridine-2-thiolate or benzothiazol-2- thiolate bridging ligands which contain the Pt-Pt bond, were reported. The complexes have relatively stable crystal structures in the dichloromethane solution and the present Pt-Pt chemical bond in the complexes lead to form the σ* HOMO contributing to the complexes optical and electrochemical processes [13].

1.2. Antitumor activity of Platinum Complexes

Platinum compounds are important chemotherapy drugs used to treat cancers. The interest in platinum based antitumor drugs has been started with the serendipitous discovery of the inhibition of cell division by platinum complexes. Among them, cisplatin, cis-diamminedichloroplatinum(II), was approved by United Sates FDA as an antitumor drug in 1978 [14]. Because of the high activity of Cisplatin against testicular and ovarian cancer, it has been used in the treatment of cancer patents frequently. Despite the success of Cisplatin chemotherapy, it has several serious side effects such as nausea, vomiting, nephrotoxicity, ototoxicity, neuropathy and myelosuppression [15-

23]. The other main reason for a failure of cisplatin chemotherapy is resistance of tumors to the drug. The resistance can be intrinsic or acquired and limits the applicability of cisplatin [24-25].

Cisplatin Transplatin

Figure 1. Structure of the antitumor drug, cisplatin, and its inactive trans isomer, transplatin.

Today, improving on existing chemotherapy is essential to both increase the spectrum of tumors that can be cured and to increase the quality of life of the patients undergoing treatment.

Twenty- five years after the first discovery of cisplatin, the second and third generation platinum drugs carboplatin, cis-diammine(1,1-cyclobutanedicarboxylato)platinum(II), and (trans-R,R-cyclohexane-1,2-diamine) oxalatoplatinum(II) as oxaliplatin, are utilized in clinical trial [15,26]. The carboplatin and the other platinum drugs of the second- generation were created by backing off the rate of reactions with bidentate X_2 ligands, to reduce the dose limiting harmfulness of cisplatin. It was created by replacement the exchangeable chloride ligands with a bidentate 1,1-cyclobutanedicarboxylic acid ligand and this reduces the toxic effect of drugs and makes it suitable for high – dose administered [15,23].

The third generation platinum complexes were described to overcome the cell resistance against to cisplatin and carboplatin. Oxaliplatin has also a high potential as a treatment choice after failure of cisplatin and carboplatin treatment. The clinical activity of oxaliplatin has been accounted in ovarian and germ-cell cancers. Also, oxaliplatin is less toxic than cisplatin and carboplatin [27].

In the last decades, some platinum compounds containing aromatic amines and amino acids with dithio carbamate derivatives were synthesized to reduce the side effects of the platinum based drugs. In order to increase the solubility of the platinum complexes in aqueous solutions the chloride anion replaced with a chain aliphatic carboxylate group or a cyclocarboxylate group [23,38].

Heidari et al. prepared new platinum (II) complexes that contains the drug metformin and DMSO ligand similar to the cisplatin complex and expected to point out antitumour activity by interaction with DNA and BSA. The results suggested that Pt(II) complex with (Met) drug bounded with DNA via groove binding mode [18].

Picoplatin is the other example of the new platinum complexes which exhibited activity in lung, ovarian and prostate solid tumors in phase I and phase II clinical trial, but in phase III trials picoplatin neglected to demonstrate the efficacy in the cancer. Moreover, picoplatin has interesting feature so that its capacity to administered orally and it is the first Pt(II) drug to show great oral bioavailability and activity, and oral formulation for clinical use is awaited [23].

Similarly, 2- aminobenzothiazole ligand was used to synthesis the anticancer drugs and its complexes $[Pt(Habt)_3Cl]$ and [Pd(abt)(phen)]Cl (Habt), (2- aminobenzothiazole) (abt), (2- aminothiazole) were evaluated against breast and ovarian tumor in human cells but the results in this study showed that those complexes were more cytotoxic than cisplatin to breast and ovarian cells [28].

Although, it is well known that trans isomer of cisplatin is completely inactive towards the cancer tumors, various platinum complexes in trans geometry showing anticancer activity were reported in literature. For instance, trans-dichlorido Pt(II) complex binding two amine carrier ligands are 2-(2-hydroxyethyl)pyridine was synthesized and studied by Icsel et al. [29]. Results indicated that this trans complex has higher antitumor activity against different cancer cells than cisplatin, carboplatin and oxaliplatin.

Trans-bis(3-aminoflavone)dichloridoplatinum(II) was described as a potential anticancer compound that has a significant cytotoxic effect against human and murine

tumor cell lines as well as weaker toxicity towards healthy human peripheral blood lymphocytes compared with cisplatin [30]. This trans complex is markedly higher proapoptotic activity than that of cisplatin and its associate antineoplastic specificity is completely different from that of cisplatin.

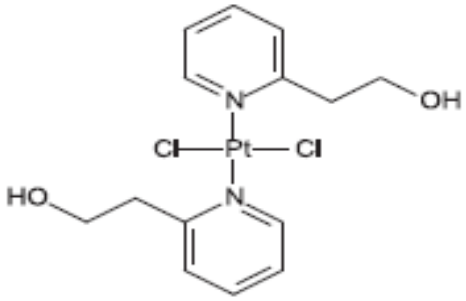

Figure 2. Trans-dichlorido Pt(II) complex with 2-(2-hydroxyethyl)pyridine

The first study on the cytotoxic impact of sulfonamide platinum complexes was reported by Del Solar et al. They synthesized a series of trans-N-sulfonamide Pt(II) complexes and studied the antiproliferatif effect of the complexes agents to the solid cancers cells in human. The most effective compound has the geometry of trans-dichloride, dansylsulfonamide and dimethyl sulfoxide (DMSO) coordinated to the central platinum metal, which emits visible radiation[31- 32].

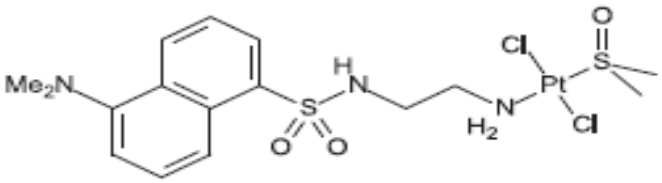

Figure 3. Trans-dichloride , dansylsulfonamide and dimethyl sulfoxide.

A new platinum (II) complex known as Pt-trp (-Pt tryptophan) which was synthesized and characterized by S. Shishido et al. with a 1:2 molar composition (metal: ligand) was obtained. Mass spectroscopy, infrared measurements as well as ^{15}N and ^{13}C

NMR spectroscopic information within the solid state indicated coordination of the ligand to Pt(II) through the nitrogen of the NH_2 group additionally the oxygen of carboxylate group in the square planar geometry around the metal center [33]. They studied Pt(II) with tryptophan , with emphasis on its possible it use as anticancer agent and it showed that Pt-trp was less toxic than cisplatin.

1.3. Platinum Blues

Platinum blues are intresting compounds due to not only of their high antineoplastic activities, but also for their unusual navy blue color. In general, intensely colored platinum compounds owe this feature to intervalence charge transfer transitions, because of the presence of different oxidation states of platinum. Among the colored platinum compounds, those containing amide and\ or amidate ligands have received attention for about100 years [15].

The first "platinum blue" complex was prepared in 1908 by the reaction of yellow cis-$Pt(II)Cl_2(CH_3CN)_2$ with Ag_2SO_4. Despite the fact that the resultant compound was proposed initially as a mononuclear of $Pt(II)(CH_3CONH_3).H_2O$, later it was reported that the product is a polymeric platinum complex with bridging acetamidate linkages (Figure 4) [38].

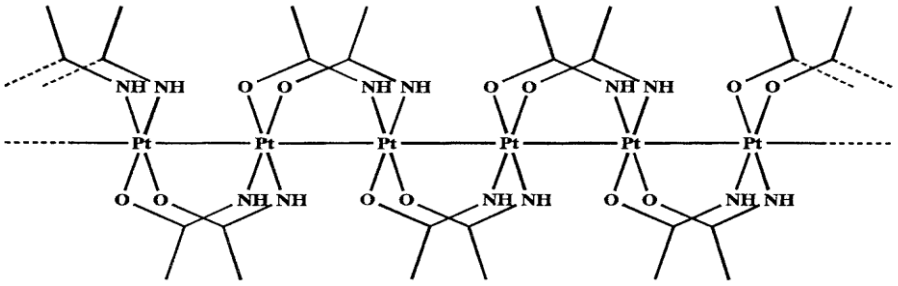

Figure 4. A possible polymeric structure of the original $Pt(CH_3CONH)_2$ system.

Numerous platinum blues complexes have been prepared by using K_2PtCl_2 as a starting material with a variety of amide ligand. Several structures have been assigned to the platinum blues due to the problem of the isolation of their crystalline form. A square planar and chelating acetamide groups generally are accepted as the most stable structure of those complexes. However, the alternative structures those contain six-coordination dimers and polymeric chains with acetamido as the bridge is also proposed [34]. Another important feature of such compounds is the mixed oxidation state of the platinum ions in their oligomeric structure besides their distinctive color. The common Pt oxidation state in octanuclear "Pt acetamide blue" array, for instance, is 2.25 with the formal description of $[Pt^{2.0}]_2[Pt^{2.5}]_4[Pt^{2.0}]_2$ justified on the basis of Pt-Pt. The actual structure could be further complicated by different orientations of the bridging acetamidates (head-to head, *h-h* or head to tail, *h-t*) [15].

Cis-diammine platinum α-pyridone blue was the first crystalline platinum blue and its structure [35], chemical and physical properties were fully described. Almost all platinum blues are originated from the amidate-bridged structures containing mixed valent platinum ions. Only a few of them comprise metal-metal bonded oligomers of altering chain lengths [36].

Using carbazide based ligands such as 1-phenylthiosemicarbazide, 1-4 diphenylthiosemi carbazide, 4-phenylthiosemicarbazide, 4-(2-pyridyl)-thiosemicarbazide new platinum blue complexes were also synthesized very recently [34], where N and S-donor atoms were in trans positions to the each other. The blue color of the complexes was attributed to low energy electron transition from the a_{1g} metal orbital to the a^*_{2u} ($d\pi^*$) orbital of sulfur and HOMO of the metal was close to the antibonding LUMO of sulfur in the platinum complexes with thiosemicarbazide ligand.

The blue color of most platinum blue complexes is attributed to the mixed valent character platinum atoms in their oligomeric structures but the observed of bands of maximum absorption is not uncommon; the metal to ligand charge transfer band which is observable at around 650-750 nm region in the electronic absorption spectrum of all platinum blue complexes, is attributed to their blue color [34].

Special attention was paid to the platinum blues produced from the reactions between the hydrolysis product of cisplatin (i.e., cis-$[Pt(NH_3)_2(OH_2)_2]^{2+}$) and pyrimidine bases such as uracil, since these so-called "platinum-pyrimidine-blues" were found to have a high index of antitumor activity with a lower associated nephrotoxicity than cis-DDP [37].

1.4. The Aim of the Study

A novel platinum blue complex containing 2-aminothiophenol (2-atp) (**1**), $[Pt_4(2\text{-}atp)_8(H_2O)(OH)]$, was synthesized and characterized before in our group [38]. Various platinum blue complexes containing nitrogen and oxygen have been synthesized, however, no platinum blues compound containing sulphur and nitrogen has been reported until that study.

The main objective of this study is to synthesize new platinum blue complexes by using sulphur donor ligands, 2-aminothiophenol via different experimental methods and conditions. Analysis of the products is performed by comparing the molar absorptivity constants of newly generated platinum blue complexes with the one reported by Erilhan and his coworkers [38].

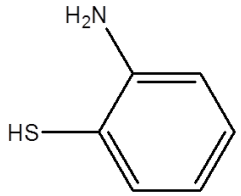

Figure 5. Molecular structures of 2-aminothiophenol (**1**)

DNA binding ability of the platinum blue complex was studied by spectroscopic methods. In order to determine the binding mode of platinum blue complex, the spectral change is followed in the electronic absorption spectrum of the complex in the presence of the calf thymus DNA. Viscometric and fluorometric methods were also employed to clarify the effect of the complex on the DNA.

CHAPTER 2

EXPERIMENTAL SECTION

2.1. Synthesis of complexes

In order to understand the effect of the experimental conditions and the initial material to prepare a new platinum blue complex, four different reaction conditions were studied starting from cisplatin.

2.1.1. Procedure [I]

50 mg (0.2174 mmol) of cisplatin was dissolved in 5 ml of water and 0.0739 mg (0.435mmol) of $AgNO_3$ was added directly to this aqueous platinum solution. The mixture stirred over night at room temperature at dark. Then the yellowish solid was filtered out. The pH of the filtrate was adjusted to 13 by adding NaOH. After that, 47.88µl (0.4348mmol) of (2-atp) was added to this basic solution by stirring. In order to increase the solubility of 2-atp in aqueous solution 1 mL of DMF was added to the mixture. Then, the solution is neutralized by adding HCl. The resultant neutral mixture refluxed at 40º C for 3 h. A dark blue solid precipitate formation was observed. After the reflux process, the solution was kept in refrigerator overnight and then the solid is collected by filtration and dried at room temperature under vacuum.

2.1.2. Procedure [II]

To the 5 ml basic (pH=13) aqueous solution of 50 mg(0.2174 mmol) of cisplatin, 23.94µl (0.2174 mmol) of (2-atp) was added directly by stirring. In order to dissolve of 2-atp in this aqueous solution, 1 mL of DMF was added to the mixture. Then the pH of the solution was adjusted to 7 by adding HCl solution and then refluxed at 40º C for 3 h. A dark blue solid precipitate formation was observed. After the reflux process, the solution was kept in refrigerator overnight and then the solid is collected by filtration and dried at room temperature under vacuum.

2.1.3. Procedure [III]

To the 5 ml aqueous solution of 50 mg (0.2174 mmol) of cisplatin, 23.94µl (0.2174 mmol) of (2-atp) was added directly by stirring without making the solution basic. In order to dissolve of 2-atp in this aqueous solution, 1 mL of DMF was also added to the mixture. Then the solution is refluxed at 40º C for 3 h. A dark blue solid precipitate formation was observed. After the reflux process, the solution was kept in refrigerator overnight and then the solid is collected by filtration and dried at room temperature under vacuum.

2.1.4. Procedure [IV]

50 mg (0.2174 mmol) of cisplatin was dissolved in 5 ml of water The pH of the solution was adjusted to 13 by adding NaOH. Then, 47.88µl (0.4348 mmol) of (2-atp) was added to this basic solution by stirring. In order to increase the solubility of 2-atp in aqueous solution 1 mL of DMF was added to the mixture. Then, the solution is neutralized by adding HCl. The resultant neutral mixture refluxed at 40º C for 3 h. A dark blue solid precipitate formation was observed. After the reflux process, the solution was kept in refrigerator overnight and then the solid is collected by filtration and dried at room temperature under vacuum.

2.2. DNA Binding of Platinum Blue

2.2.1. Spectroscopic measurements

Electronic absorption spectra were monitored using a HP Agilent 8453 spectrophotometer. The change in the electronic absorption spectrum of the Pt-blue complex was followed by keeping the concentration of complex constant (2.13×10^{-5} M) while increasing the concentration of Calf Thymus DNA (ct-DNA) from 0-2.13×10^{-3} M (R=[DNA]/[Complex]=0-10). The best incubation time for the DNA-Drug interaction was observed as 30 minutes at 37^{o}C spectroscopically. The intrinsic binding constant (K_b) of Pt-blue with CT-DNA was determined at 555 nm using the following equation [39, 40];

$$[DNA]/(\varepsilon_a-\varepsilon_f) = [DNA]/(\varepsilon_b-\varepsilon_f) + 1/K_b(\varepsilon_b-\varepsilon_f), \qquad (1)$$

Where ε_a is the apparent extinction coefficient, is expressed as A_{obs}/[Pt-Blue], ε_b and ε_f represent the extinction coefficients of free and the bound complex, respectively. K_b is calculated from the ratio of the slope to the intercept obtained in a plot of [DNA]/(ε_a-ε_f) vs [DNA].

In order to understand the nature of the interaction between the Pt-blue complex and ct-DNA, thermodynamic experiments were performed and the temperature dependent binding constant (K_b) was determined at 310, 320, 330 and 340 K.

DNA melting experiments were carried out following the change in the electronic absorption spectrum of CT-DNA at 260 nm between 30-90^{o}C (1^{o}C/1 min) in the presence of the complex and DNA alone.

Viscosity measurements were carried out using a viscometer (AND-Vibroviscometer SV-10) at room temperature. Viscosity of the CT-DNA in presence (η) and the absence (η_o) of the complex was measured automatically. Data were presented $(\eta/\eta_o)^{1/3}$ versus 1/R[41,42].

Fluorometric measurements were performed with Thermo Scientific Lumina Fluorescence Spectrometer by keeping the ethidium bromide pretreated ct-DNA

concentration constant by varying the complex concentration between 0 to 160 µM. Stern-Volmer Constant (Ksv) [39,43] was determined from the following equation;

$$F_o/F = 1 + K_{sv}[Q], \quad (2)$$

Where F_o and F represents the emission intensities in the absence and the presence of the quencher (Q), respectively. K_{sv} was determined from a plot of F_o/F versus [Q] ([Q] = concentration of quencher).

All spectroscopic measurements were carried out in 1:1 (v/v) mixture of 5 mM Tris-HCl (pH=7.1) and 50 mM NaCl buffer solution.

All experiments were performed at least three times with similar results.

2.3. Cytotoxicity

All cytotoxicity experiments were carried out by our colloborators, group of Dr. Ceyda Açılan Ayhan, in TÜBİTAK Marmara Research Center.

2.3.1. Agarose gel analysis of Pt-Blue complex/DNA interactions

DNA / Pt-blue complex interactions were analyzed in-vitro under the following conditions: 100 ng purified plasmid DNA (actin-GFP cloned into pcDNA3.1) was incubated with 20 µM, 40 µM and 80 µM concentrations of the Pt-blue and cisplatin simultaneously (Pt-blue and cisplatin drugs were dissolved in ddH2O). Another set of 40 µM and 80 µM complex-DNA reactions were set with additional 2.5 µl 2% NaN_3 (in ddH_2O) to inhibit ROS formation upon complex-DNA interaction. Samples were incubated for 20 h at RT. 100 ng plasmid DNA was also digested with BamHI (MBI Fermentas) to observe the linear DNA on 1% agarose gel. DNA bands were visualized under UV transilluminator (UVITEC Cambridge).

2.3.2. Cell culturing

All cells were maintained in Dulbecco's Modified EagleMedium/F12 (DMEM/F12, Sigma-Aldrich, #D0547) supplemented with 5% FBS (Biochrom, #S0415), and penicillin (100 units/ml)-streptomycin (100 µg/ml) (Biochrom, #A2212) at 37ºC in 5% CO_2. Cells were harvested using Trypsin (Biological Industries, ♯03-053-1).

2.3.3. Treatment of cells with the Pt-blue complex and determination of cell viability

All cells were seeded on 96-well plates and cover slips and incubated for 24 h, at cell culture conditions. Pt-Blue complex (Pt4(2-atp)8(H_2O)(OH)] (2-atp: 2-aminothiophenol)) was freshly prepared at 10, 20, 40 and 80 µM concentrations and added on to the cells, which were further incubated for 24, 48, 72 h. Cell viability was determined using WST-1 agent (4-[3-[4-iodophenyl]-2–4(4-nitrophenyl)-2H-5-tetrazolio-1,3-benzene disulfonate]) (Roche, Cat # 11644807001) as described in [67].

2.3.4. DNA condensation/fragmentation analysis

MDA-MB-231 or MDA-MB-435 cells were seeded on 12 mm cover slips (6×10^4 cells), and incubated for 24 h. The following day, 20 and 40 µM complex was freshly prepared, added on the cells and further incubated for 24 or 48 h. Cells were fixed in -20^{o}C methanol, and the DNA was counter stained using DAPI. Images were taken using Leica DMI 6000 fluorescence microscope using the same camera settings.

2.3.5. Live cell imaging microscopy

2×10^5 cells were cultured on 35 mm plates and incubated for 24 h at 37°C, 5% CO_2. Next day, freshly prepared Pt-blue complex was added on cells, and the plate was immediately placed under the microscope. Images were taken as described in [68, 69].

2.3.6. Detection of total ROS via 2', 7'–dichlorofluorescein diacetate (DCFDA)

Cells were seeded on 96-well plates or 12 mm cover slips in culture media, and incubated for 24 h at 37ºC in 5% CO_2 [52]. Next day, 10, 20, 40 or 80 µM of the Pt-blue complex was freshly prepared, added on cells and further incubated for 24 or 48 h. Following one PBS wash, 5 µM of DCFDA (Sigma, Cat # D6883) agent was added on cells for 30 min at 37ºC. 96 well plates were read at 485 nm (excitation), 535 nm (emission) wavelengths using a microplate reader (Biotek Instruments Inc.). Fluorescein intensity was normalized for cell number.

2.3.7. Immunofluorescence staining

6×10^4 cells were seeded on 12 mm cover slips and incubated for 24 h at 37ºC in 5% CO_2. The following day, 20 and 40 µM of the Pt-Blue complex was freshly prepared and added on the cells for 24 or 48 h and fixed with 4% paraformaldehyde/PBS (15 min at room temperature (RT)). Cells were permeabilized using 0.3% Triton X-100/PBS (15 min, 4^oC) and blocked with 0.2% gelatin/PBS (1 h at RT). Cells were stained using γH2AX antibodies (Cell Signaling, #9718S, diluted in 0.2% gelatin/PBS, 1:400), or 8-oxo-Guanine antibodies (EMD Millipore, MAB3560, 1:100) at 4ºC, overnight and secondary antibodies (Abcam, #97068, 1:250, 2 h at RT). Cover slips were flipped onto mounting medium containing DAPI. Cells were imaged using Leica DMI 6000 fluorescence microscope using the same camera settings at 100X magnification.

2.3.8. Tunel

Cells were treated with the indicated doses of the Pt-blue complex for 24 h, fixed in 4% freshly prepared paraformaldehyde and stained using in situ cell death detection kit (Roche, TUNEL-POD) without any modifications using manufacturer's protocols as described in [67].

2.3.9. Real-time PCR analysis

MDA-MB-231 cells were treated with 20 μM of the Pt-blue complex and lysed 48 h after treatment. RNA was isolated following the protocols and reagents in the NucleoSpin RNAII kit (Macherey-Nagel) without modification. cDNA was synthesized with 1000 ng of total RNA using iScript cDNA synthesis kit (Bio-Rad Laboratories) in a total of 20 μl/reaction. RT-qPCR was performed using Bio-Rad iQ5 PCR Thermal Cycler using SYBR Green Supermix (Bio-Rad Laboratories). Custom array primers were obtained from Sentegen Biotech. The array was run in duplicate. For genes that showed significant change (≥ 2 fold), a total of 3 biological repeats were performed, all in duplicate. The expression of genes that showed the same trend in all experiments (up or down regulation) was only considered a real difference. To confirm specificity of the amplification, melting curves were analyzed individually for all runs, and runs that showed primer dimers were eliminated from analysis.

CHAPTER 3

RESULTS and DISCUSSION

3.1. Preperation of Platinum Blue

Figure 6 demonstrates the ball and stick model and the chemical structure of the Pt-blue complex, $[Pt_4(2\text{-atp})_8(H_2O)(OH)]$, used in this study. The synthesis and the analysis of the compound was reported by our group previosly [44] and was found to be >95% pure based on Elemental analysis, UV-Vis, IR, ESR, ESCA, SEM, 1H-NMR, 13C-NMR, 195Pt-NMR and electrochemical analysis [38]. However, the complex was not evaluated previously for its interactions with DNA. Hence in this report, we further studied the properties of this complex based on its effect on DNA.

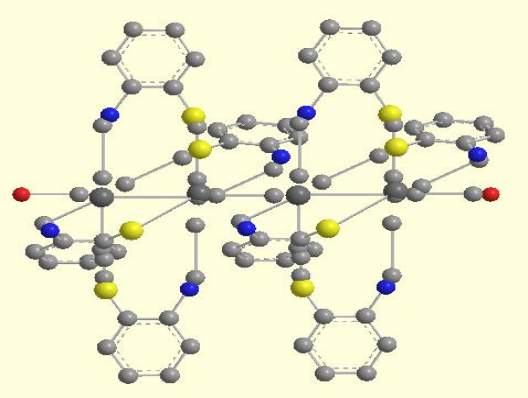

Figure 6. Ball and stick model of the platinum blue complex containing 2-atp.

Four different experimental procedures were performed by using cisplatin as a starting platinum source unlike our previous mentioned work in which, potassium tetrachloroplatinate was used as an initial platinum supplier. Basicity as well as metal to ligand ratio was changed as 1:1 or 1:2 in order to synthesize possible novel platinum blue complexes containing both 2-atp and NH_3 ligands. However, comparative electronic absorption spectrum studies with that of $[Pt_4(2\text{-atp})_8(H_2O)(OH)]$ surprisingly indicated the formation of the identical complex in each trial.

3.2. Electronic Absorption Spectroscopy

Electronic absorption spectroscopy is used to demonstrate the interaction of platinum blue with ct-DNA. Intercalation of metal complexes to ct-DNA generates hypochromism and red shift as a result of strong interaction between an aromatic group of a ligand and a base pair of DNA. However, the intensity of the band at 555 nm increased obviously with an insignificant shift after the addition of the increased amount of ct-DNA as depicted in Figure 7.

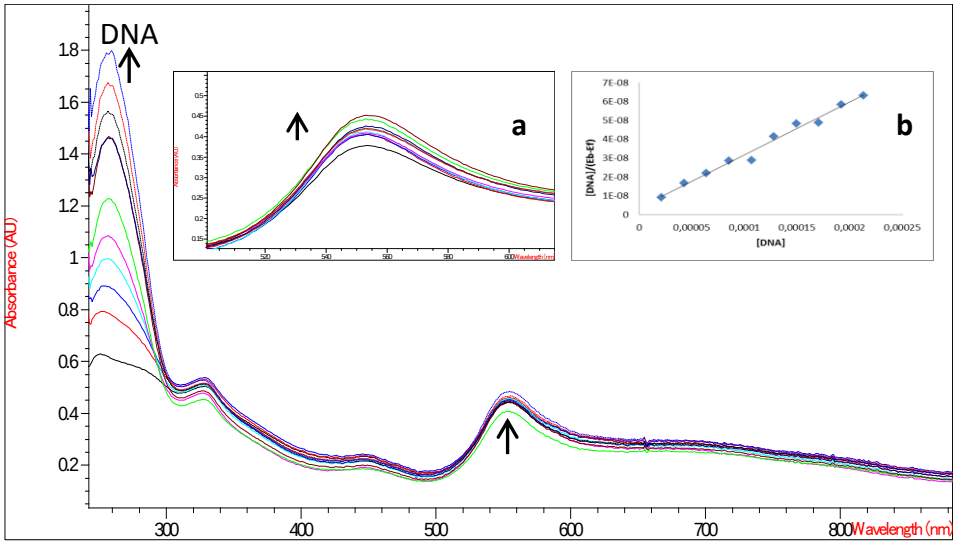

Figure 7. Electronic absorption spectrum of Pt-Blue complex in the presence DNA at pH=7.1 in 5 mM Tris-HCl buffer. [DNA]= $2.13x10^{-5}$-$2.13x10^{-4}$ M (R=1-10). Inset: (a)

Spectral changes observed at 555 nm. (b) Linear plot of for the calculation of intirinsic binding constant, K_b.

The observed hyperchromic effect may indicate an electrostatic interaction between the complex cation and the negatively charged phosphate groups in the double helix of ct-DNA [45] after releasing the counter ion from the axial position. In the present study, on the other hand, the partial intercalation of the aromatic groups (2-aminothiophenol) of the Pt-blue should also be considered.

The intrinsic binding constant (K_b) of the platinum complex with DNA is calculated from the changes in the electronic absorption of the strong metal to metal electronic transition band of Pt-blue at 555 nm [38] with increasing DNA concentration (Figure iset of 7). Kb value is calculated as $1x10^5$ M^{-1}. This value is less than the K_b values reported in literature for the classical intercalators; such as for ethidium bromide K_b is $7x10^7$ [46]. On the other hand K_b value of platinum blue is close to that of proflavin (4.1x105 M^{-1}) [47], some ruthenium ($1.24x10^5$) [48], copper ($1.35x10^5$, $1.23x10^5$ and $8.3x10^4$) [49] and cobalt ($9.0x10^5$) [50] complexes which are cited as an intercalator or a partial intercalator.As it is expected, K_b value of mode but in weaker extend than that expected due to the steric effect of four platinum platinum blue is at least ten times higher than K_b values for some of the DNA groove binder complexes of ruthenium chromium[51]and Zinc [49]. These results suggest that Pt-blue binds to DNA by intercalating containing chain structure of the complex.

In order to understand the nature of interaction between Pt-blue and DNA, the temperature dependent binding constant is also calculated and data is presented in Table 1. The standard Gibbs Free Energy is calculated by using the equation (3);

$$\Delta G^o = -R\ T\ \mathrm{Ln}K_b \quad (3)$$

The binding enthalpy (ΔH^o) and entropy (ΔS^o) of Pt-Blue is calculated by using slope and intercept of the van't Hoff [50] equation (4);

$$\mathrm{Ln}\ K_b = (-\Delta H^o/RT) + (\Delta S^o/R) \quad (4)$$

The negative value of ΔG^o reveals a spontaneous process (Table 1) with negative ΔH^o and ΔS^o values. The ΔH^o and ΔS^o values of the complex-DNA are -61.80 kJ/mol and −101,40 J/mol K, respectively. Generally negative enthalpy and entropy changes indicate van der Waals interactions and hydrogen bonding as a binding mode of a drug to DNA [52, 53] and hence confirm an intercalative mode of action [43]. Thermodynamic data presented in Table 1 are lower than those of previously reported ones [54]. Under the light of the obtained results, one can say that an electrostatic interaction of the positively charged complex and DNA is followed by an intercalative binding [55]. Intercalation of the 2-atp ring of ligand in complex which involves π-stacking interaction between these planar substituents and DNA base pairs are consistent with the enthalpy and entropy changes. Intercalation of two phenyl rings of the ligand between the DNA base pairs is less favorable due to the steric effect of long chain of the Pt-blue structure [56].

Table 1. Binding constant and thermodynamic parameters of platinum blue complex in Tris HCl buffer.

Temperature (^{o}C)	**K_b (M^{-1})**	**ΔG^o (kJ/mol)**	**ΔH^o (kJ/mol)**	**ΔS^o (J/mol.K)**
37	**100000**	**-29,67**	**-61,80**	**-101,41**
47	**70000**	**-29,68**		
57	**55555**	**-29,97**		
67	**10000**	**-26,04**		

3.3. Thermal stability

The thermal behavior of DNA in the presence and the absence of Pt-blue complex are studied in order to give an insight to the conformational changes of DNA-helix and the strength of DNA-complex interaction [57,58]. It's well known that, when the temperature of the solution increases the double stranded DNA gradually dissociates to

single strands by intensifying the electronic absorption band at 260 nm. The melting temperature, Tm, of DNA is characterized the transition from double stranded to single stranded nucleic acid [59] and the interaction of the complexes generally results a rise in T_m.

Therefore, Tm provides valuable information to study DNA-complex interaction. Figure 8 depicts the change in the melting curve of DNA in the absence and the presence of Pt-Blue.

The results indicate that the Tm of ct-DNA is around 76 ^oC in tris-buffer at pH 7.1. However, T_m increases to 81^oC in the presence of Pt-Blue. This result again suggests that Pt-Blue interacts with DNA strongly but the extent of changes in Tm value (ΔT_m=5 ^oC) is smaller compared to that were reported for the classical intercalators [60, 61] and hence confirm the electrostatic/intercalative binding mode of the Pt-Blue complex.

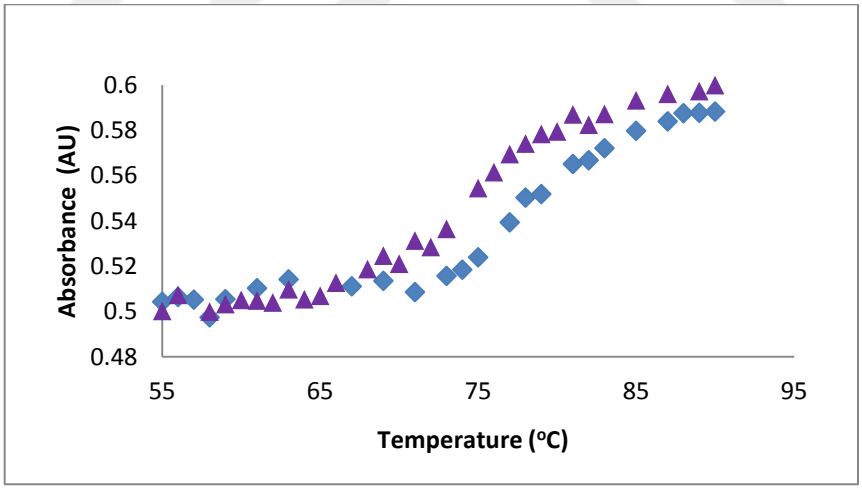

Figure 8. Thermal denaturation plot of ct- DNA in the presence (♦) and absence (▲) of Pt-Blue at different temperatures.

3.4. Viscosity study

The viscosity measurements of CT-DNA are considered as the clearest and the most critical test for determining a DNA binding mode [62,63]. A classical intercalation model would cause lengthen in DNA helix by affecting separation of base pairs and resulting in increase in viscosity.

The values of relative specific viscosity $(\eta/\eta_0)^{1/3}$ (where η_0 and η are the specific viscosity contributions of DNA in the absence and in the presence of the Pt complex, respectively) are plotted against 1/R (R= [DNA]/[complex]). In this study, it is observed that increasing the complex concentration leaded to an increase of the DNA viscosity with a slope of 0.07 (Figure 9). On the other hand, the relative viscosity reaches to 1.4 with a slope close to 1 for the classical DNA intercalator like ethidium bromide [57]. These results suggests other type of interaction(s) between DNA and the Pt blue complex such as electrostatic or hydrogen binding, which may result a decrease in the slope of relative viscosity. It should be noted that the DNA binding constant measured for this complex is 100 times lower than those determined for ethidium bromide. Therefore, the observed low in the slope of the relative viscosity of the Pt-blue-DNA adduct compared to that of DNA-EB can be associated with the lower binding constant of the platinum complex.

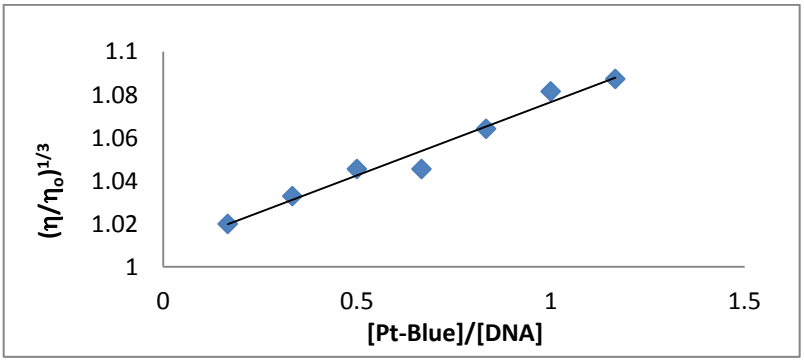

Figure 9. Effect of increasing quantity of Pt-Blue on the relative viscosity of 60 µM ct-DNA at 37 ^{o}C in 5 mM tris-HCl buffer (pH=7.2).

3.5. Fluorometry

The nature of interaction between metal complexes and DNA can be explored by florometrik titration experiments, as well. Ethidium bromide, EB, emits intense fluorescence in the presence of DNA due to its strong intercalation between the adjacent DNA base pairs. However, it was previously reported that the enhance florescence could be inhibited by the addition of another molecule [64, 65].

The quenching extends of fluorescence EB pretreated DNA can be used to determine the binding strength of Pt-Blue to DNA. The fluorescence quenching curves of EB bound DNA in the absence and the presence of Pt-Blue is shown in Figure 10.

The addition of the complex to EB substituted DNA cause a substantial decrease in emission intensity with a red shift of 10 nm, suggesting that the complex bind to DNA and exchanges with EB. These results are clearly indicative of the intercalative interaction of the platinum blue complex. Similarly, the Stern-Volmer quenching constant, K_{sq}, is obtained from the plot F_0/F vs [Pt-Blue]/[DNA] as 0.14 (inset of Figure 10), is similar to the ones reported [66] for an intercalative mode.

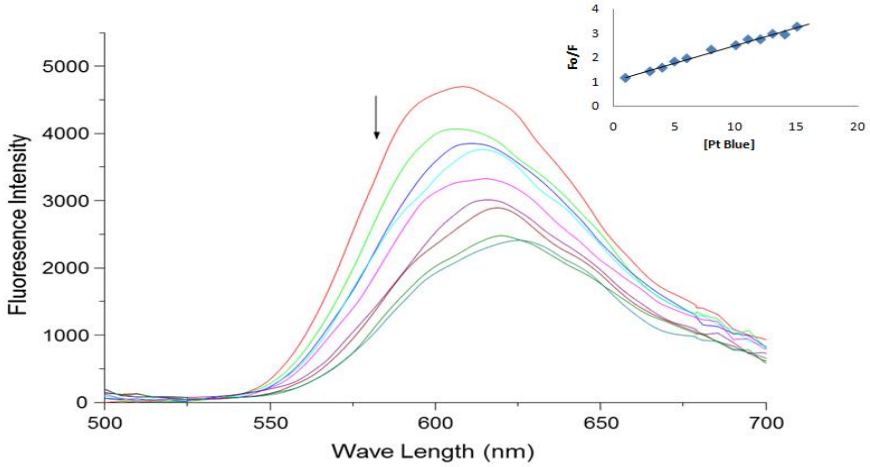

Figure 10. The change in the emission spectra of EB bound DNA upon addition of Pt-Blue in Tris HCl buffer. λex=478 nm.

Thus, fluorometric studies also support our findings and confirm an electrostatic/intercalative mode of action of Pt-Blue. It suggests that the first interaction between DNA and the Pt-Blue complex is an electrostatic interaction with the positively charged complex which is produced by exchanging the axial hydroxyl group with the solvent water, and the negatively charged DNA-phosphate back bond followed by an intercalative bonding mode [58].

3.6. Biology

3.6.1. Cytotoxicity of the Pt-blue complex

In order to evaluate the cytotoxicity and potency of the Pt-blue complex, cell viability assays were performed on a panel of cancer cells including breast (MDA-MB-231, MDA-MB-435), lung (A549), cervix (HeLa), colon (HCT116) and glioblastoma (SH-SY5Y) cancer cell lines and normal cells (primary human aortic smooth muscle cells: HASMC-1 and -2) as well as non-cancer transformed cells (CHO-K1). Metabolic activity was determined using WST-1, which is more sensitive than the MTT test; and is similarly based on the formazan product formation measuring the activity of mitochondrial enzyme succinate dehydrogenase [70]. Cells were exposed to different concentrations of the Pt-blue complex or cisplatin for 24, 48 or 72 h and dose response curves were generated (Figure 11).

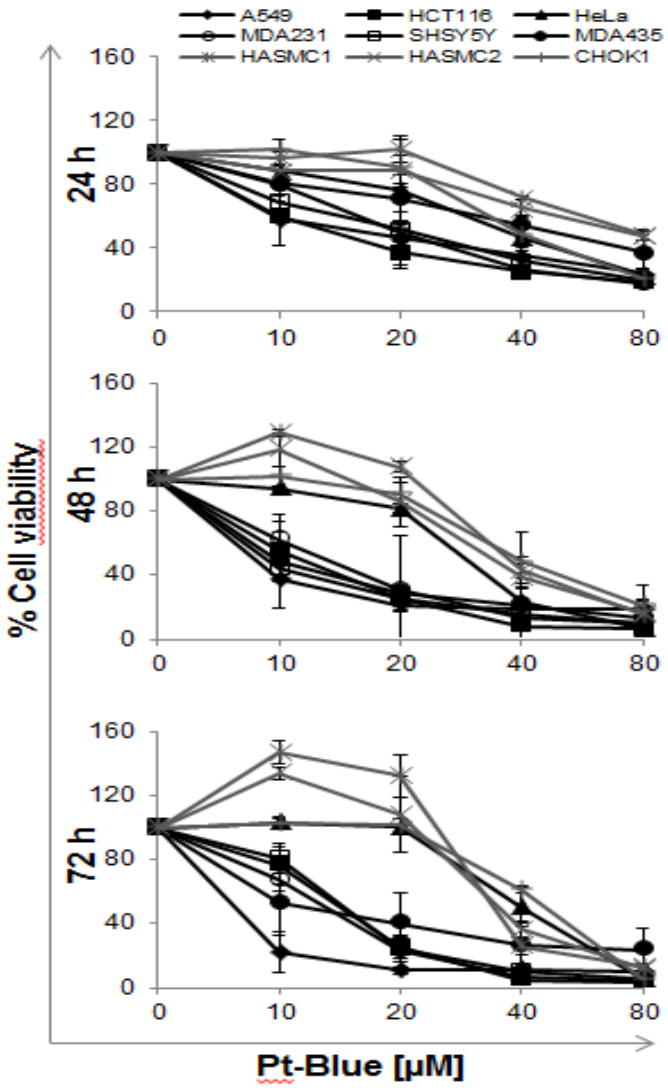

Figure 11. Cell viability graphs of cancer cells (A549, HCT116, HeLa, SH-SY5Y, MDA-MB-231, MDA-MB-435) and normal cells (HASMC1 and HASMC2) in response to different Pt-blue concentrations (0, 10, 20, 40, 80 µM) incubated for 24, 48 or 72 h.

The half maximal effective doses were deduced from the graphs and are shown on Table 2. The IC50 values were significantly lower in cancer cells, compared to non-cancer controls ($p<0,05$, Student's t test), indicating that the cancer cells were more sensitive to the Pt-blue complex. This is one of the foremost properties expected for a potential anticancer drug, and this compound appeared to be promising based on selectivity.

Table 2. IC50 values deduced from the cell viability graphs

	Cancer Cell Lines		
	24 hours	**48 hours**	**72 hours**
MDA-MB-231	27,50	21,14	22,61
MDA-MB-435	41,53	39,65	11,37
A549	18,97	10,77	8,73
HCT 116	47,39	16,13	18,11
Hela	47,39	38,92	45,52
SHSY5Y	34,85	11,89	14,74
	Non Cancer Cells		
HASMC 1	85,97	59,71	55,61
HASMC 2	75,39	42,51	36,63
CHOK1	50,89	45,40	49,67

3.6.2. Mode of cell death

In order to determine whether cells die through programmed cell death pathways (apoptosis, autophagy etc.) or through necrosis, MDA-MB-231 cells were treated with the Pt-blue complex and fixed at different times. The number of cells per frame was

greatly reduced with increasing dose and incubation times of the drug, as expected (Figure 12). We observed both fragmentation and condensation of DNA, which are hallmarks of apoptosis.

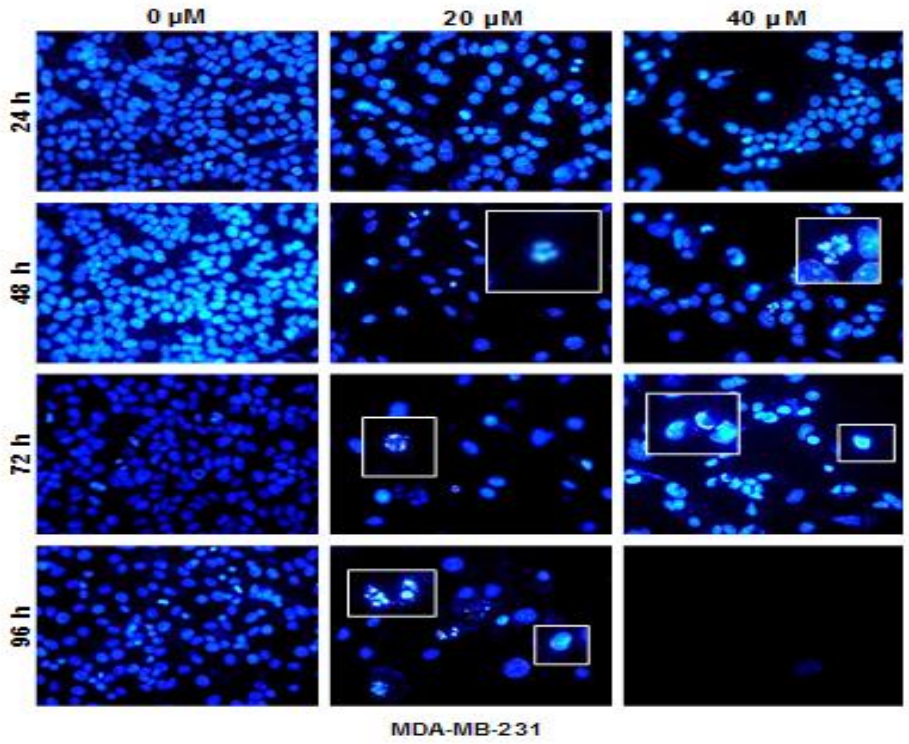

Figure 12. Nuclear morphology of MDA-MB-231 cells was observed 24, 48, 72 and 96 h after Pt-blue treatment. The nuclei were stained using DAPI. While untreated cells were increased in number and showed normal morphology, there were fewer cells per field some of which exhibited classical features of apoptosis including DNA condensation and fragmentation (see insets for enlarged view).

The results were further confirmed in MDA-MB-435 cells (Figure 13), showing similar nuclear morphologies, and suggesting apoptotic pathways.

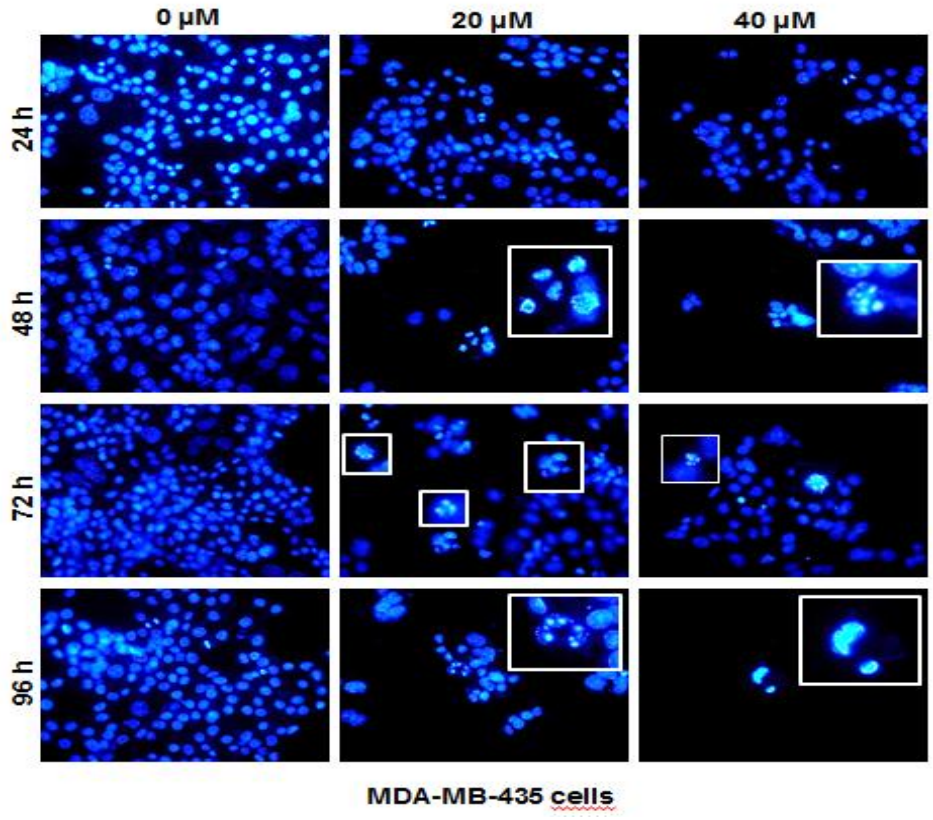

Figure 13. Nuclear morphology of MDA-MB-345 cells was observed 24, 48, 72 and 96 h after Pt-blue treatment. The nuclei were stained using DAPI. Similar to MDA-MB-231 cells, typical features of apoptosis (DNA condensation/fragmentation) were observed in MDA-MB-435 cells. Insets show enlarged view of nuclei exhibiting these features.

As the rule of thumb, several types of methods should be analyzed and evaluated together before drawing a conclusion on how cells die as a result of drug exposure. Different techniques have different drawbacks; and false positives and negatives are very common. Hence in order to further test our results, we investigated cellular morphology using live cell imaging microscopy. Cells were imaged at 5 minutes for 72 h and short movies were compiled. In accordance with previous findings, typical features of apoptosis such as cellular shrinkage, blebbing and spike formation were observed (Figure 14). Cells formed membrane blisters upon further incubation. Thus, the morphological assessments strongly indicated apoptosis as the primary form of cell death.

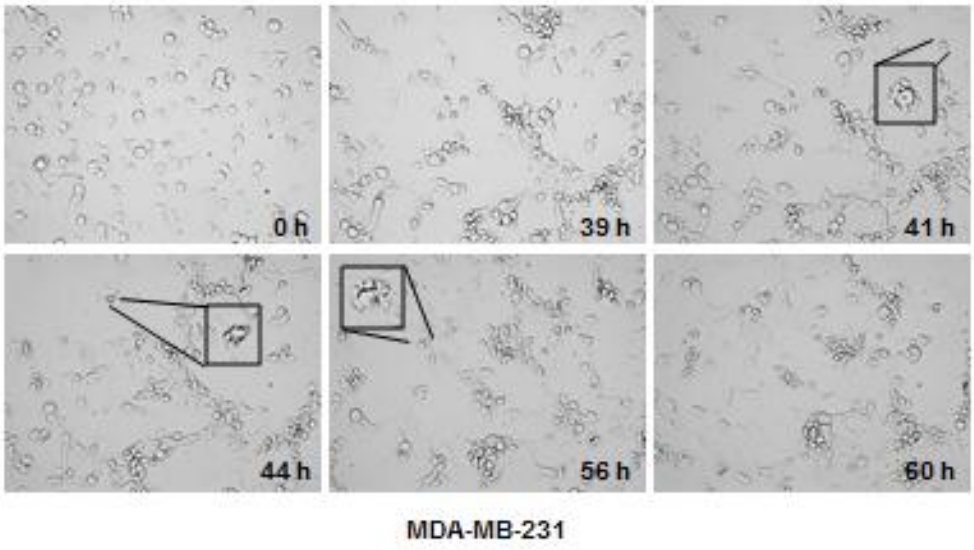

Figure 14. MDA-MB-231 cells were treated with 20 μM of the Pt-blue complex and imaged immediately at 0 h. Pictures were then taken every 5 min for 72 h and short movies were made. Images represent stills of selected time points showing characteristics of apoptosis, such as shrinkage, blebbing and spikes. Insets show enlarged views of selected cells exhibiting these features. Cells started undergoing apoptosis as early as 6 h and most. Cell death at different times is another feature of apoptosis, distinguishing it from necrosis, where most cells die all at once.

Lastly, we studied incorporation of labelled dUTPs by terminal deoxynucleotidyl transferase (TUNEL assay), which is a common method for detecting DNA fragmentation as a result of apoptosis. Similarly, cells were TUNEL positive following drug exposure, supporting apoptotic pathways (Figure 15). Hence, the Pt-blue complex appears to induce cell death through programmed pathways, mainly apoptosis, as determined by three different analyses. Since apoptosis does not induce inflammation, many debates that it should be the preferred pathway for chemotherapeutic intervention. Therefore, our compound appears to be a good prodrug candidate via induction of apoptosis in cancer cells.

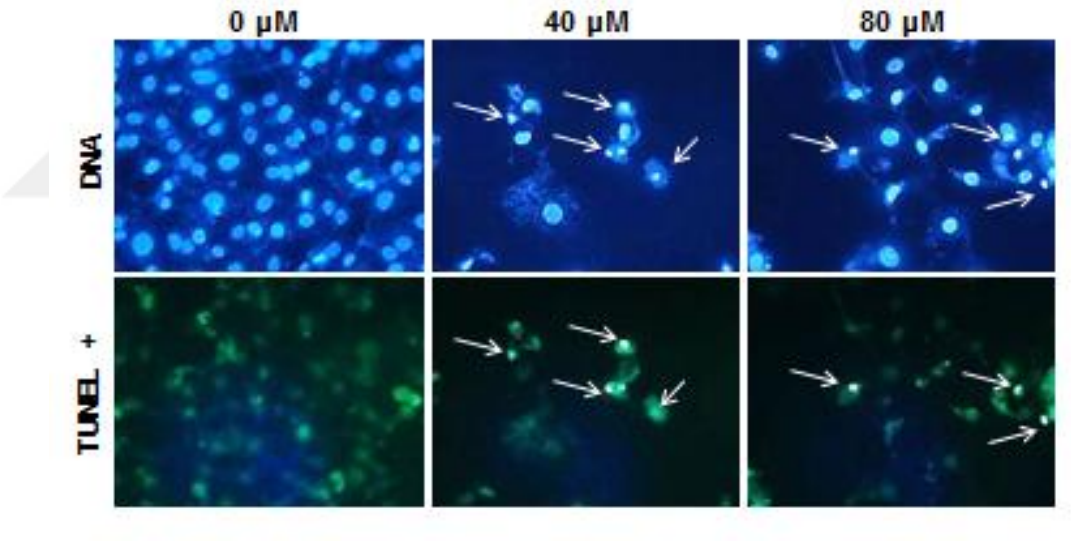

Figure 15. Terminal deoxynucleotidyl transferase end labelling (TUNEL) assay. Cells were treated with 40 or 80 µM of the Pt-blue complex and fixed after 24 h according to the TUNEL protocol. TUNEL positive cells were obtained in cells that exhibited condensed nuclei as expected, suggesting that these cells underwent apoptosis.

3.6.3. Formation of DNA breaks in cell culture

Since we observed formation of double stranded breaks (DSB) on plasmid DNA (linear form) at higher Pt-blue concentrations (Figure 16).

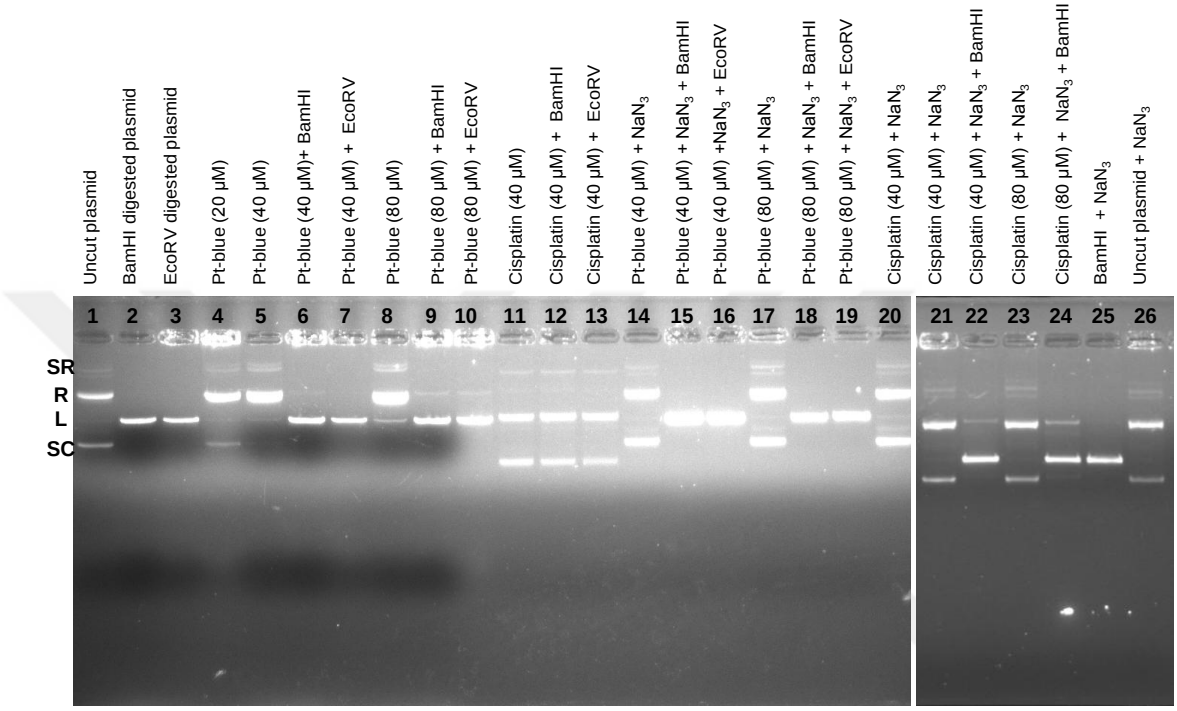

Figure 16. The changes in the migration pattern of plasmid DNA as a result of incubation with Pt-blue in comparison to cisplatin. The migration of the linear band was determined by digesting the plasmid with either Bam HI or Eco RV, which are both single cutting enzymes at the multiple cloning site. Addition of Pt-blue induced an increase in the intensity of the relaxed band and the linear band in a concentration dependent manner, indicating that single and double stranded DNA breaks were formed. Cisplatin treatment resulted in faster migration the plasmid DNA, possible due to more compact structures as a result of intercalation. Both types of DNA damage were reversed by the addition of NaN_3, a ROS scavenger. Please see text for more explanation. Two different gels are shown in the figure (lanes 1-20 and 21-26). The labels of the lanes are given on top of the gels. The bands are labelled as: SR: Super relaxed, R: Relaxed, L: Linear, SC: Supercoiled.

We wanted to test if DSBs also occurred in cells upon drug exposure. For this reason, cells were stained with γH2AX, a well-established marker for DSBs, which forms punctate foci at the sites of DNA damage [71]. As expected, cells were positive for γH2AX following Mitoxantrone treatment, which is a clinically used anticancer drug known to induce DSBs (Figure 17, bottom panel) [72]. On the other hand, there was no foci formation even at the highest drug concentrations (Figure 17, top panels), indicating that the Pt-blue complex did not induce DSBs in cells.

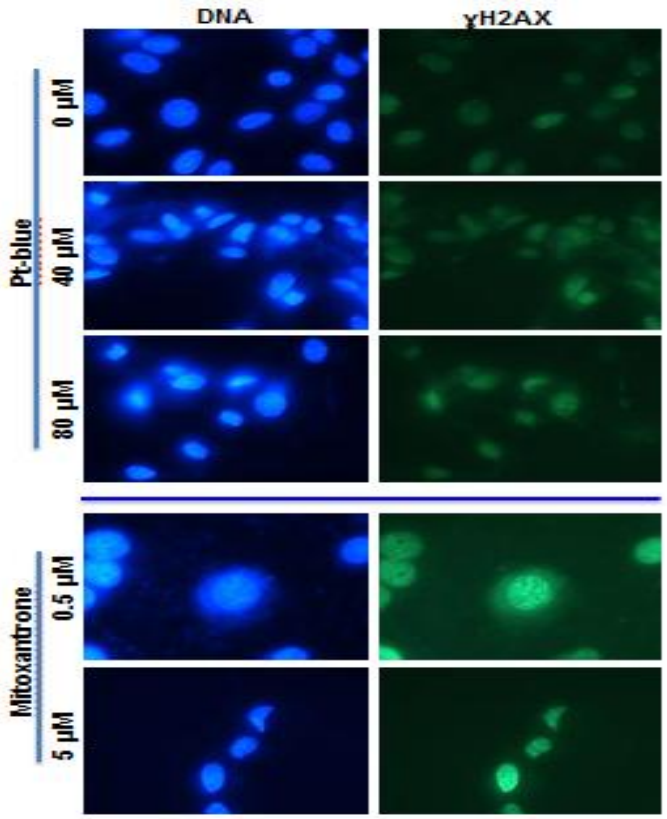

Figure 17. MDA-MB-231 cells were treated with 0, 40, 80 μM of the Pt-blue complex and fixed 24 h post treatment. While treatment of cells resulted in punctate foci following Mitoxantrone treatment, no γH2AX positive cells were observed indicating that the complex did not induce breaks in cell culture.

Similar conclusions were drawn, when MDA-MB-435 cells were used (Figure 18) and when earlier time points (4h, 8h, and 16h) were taken (Figure 19).

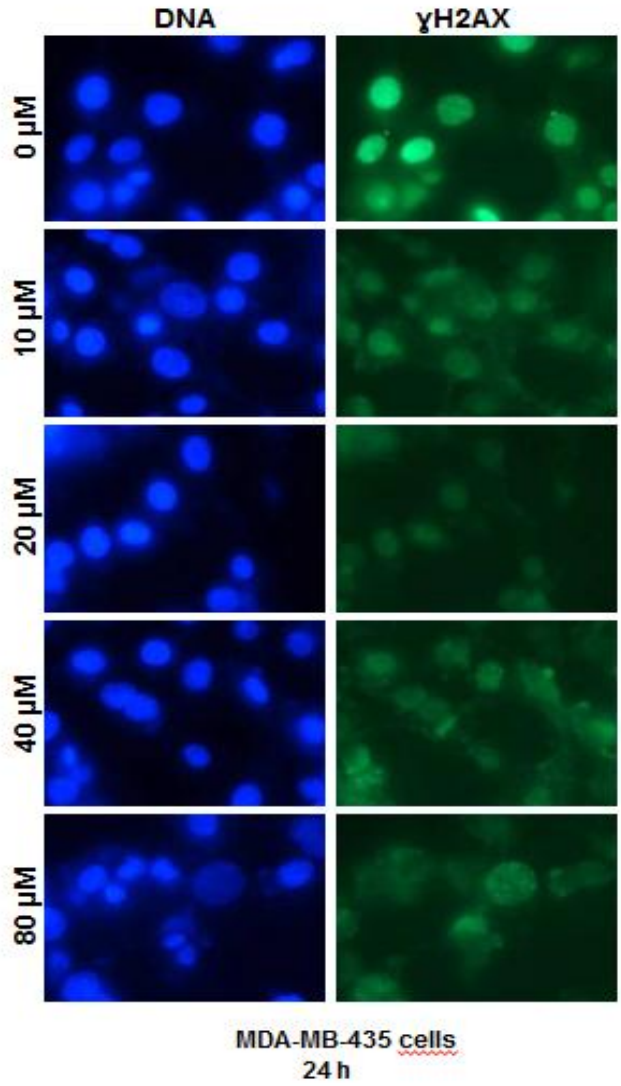

Figure 18. MDA-MB-435 cells were treated with 0, 10, 20, 40, 80 µM of the Pt-blue complex and fixed 24 h post treatment. Once again cells were negative for γH2AX, confirming that the complex did not induce breaks in cell culture

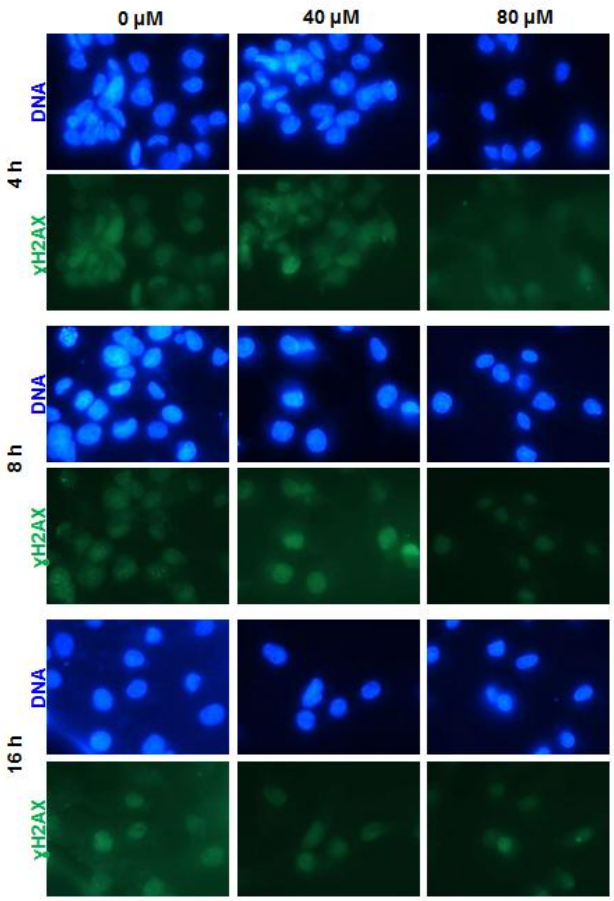

Figure 19. MDA-MB-231 cells were treated with 0, 40, 80 µM of the Pt-blue complex and fixed at several time points (4 h, 8 h, and 16 h) to test if DNA DSBs can be detected at time points earlier than 24 h. The results showed that there was no significant increase in foci formation, suggesting that the Pt-blue complex did not induce breaks in cell culture.

The difference between the in vitro plasmid assay and the cell culture system could be that the cellular DNA might never be exposed to the high concentrations of Pt-blue, which was added in the medium of the cells. The effective concentration might have been reduced by not being able to pass through cellular membranes or the drug might be efficiently detoxified by the cells. While the added concentrations of the drug were

proficient enough to produce damage and induce cell death, it did not form DSBs, suggesting that the mechanism of action is through other forms of DNA damage such as its intercalation or other oxidative effects.

3.6.4. Oxidative stress in cells

Our in vitro plasmid analysis also revealed presence of ROS during the DNA damage caused by the Pt-blue complex. In order to test this in cell culture, total ROS formation was assessed using 2',7' –dichlorofluorescin diacetate (DCFDA) which is a fluoregenic dye that is deacetylated upon entering the cell into a non-fluorescent compound. It is later oxidized to a highly fluorescent compound (DCF), upon oxidation by different forms of ROS, such as hydroxyl or peroxyl species, and can be detected using fluorometric microplate readers or fluorescence microscopy. In our analysis, we detected a significant induction of ROS in cells in response to Pt-blue (Figure 20). The increase obtained from the graph (Figure 20A), was well in accordance with the intensity observed under the microscope (Figure 20B) and the intensity was elevated with increasing doses.

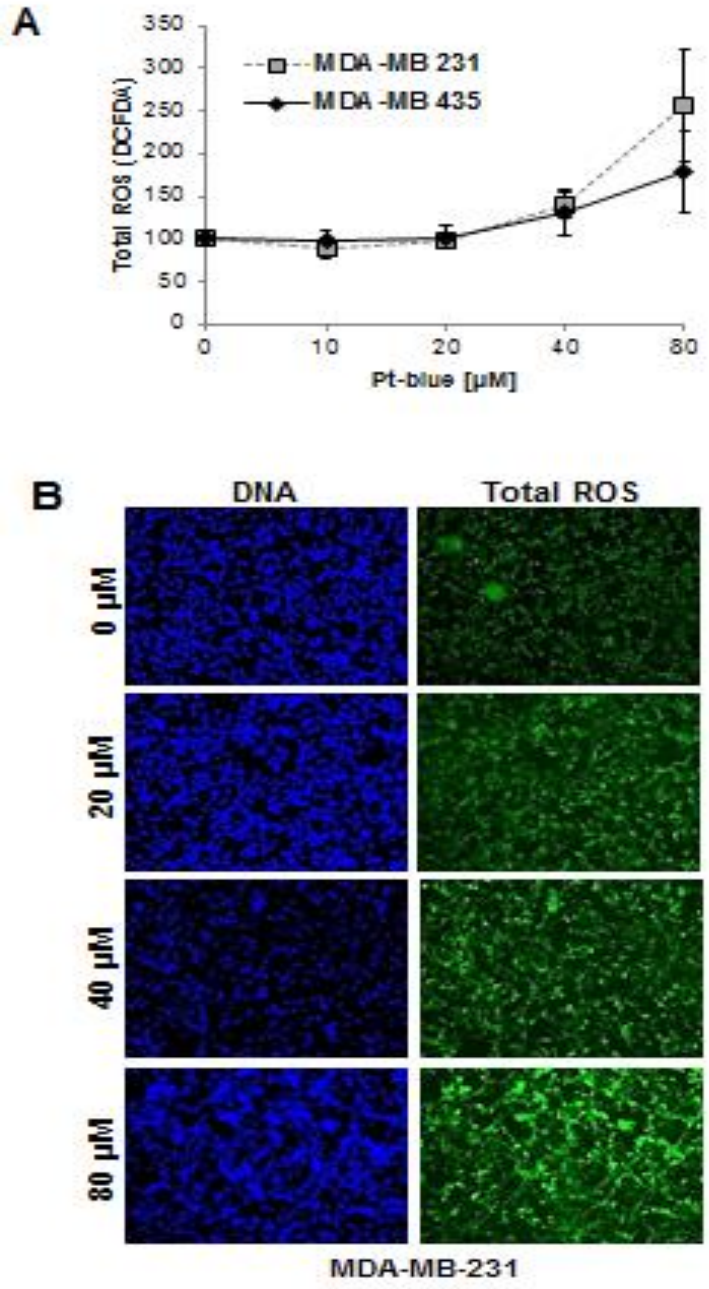

Figure 20. Cells were treated with 0, 10, 20, 40, 80 µM of the Pt-blue complex and stained with DCFDA either on 96 well plates (A) or on glass cover slips (B). DCFDA intensity was normalized for cell number (A). Results from MDA-MB-231 cells are shown in (B). All cells exhibited increase in total ROS, with varying degrees. The fluorescence intensity observed under the microscope correlated well with the dose of the drug.

To further test whether the elevated oxidative stress in cells was high enough to induce DNA damage, cells were stained for 8-oxo-Guanine, the oxidized form of guanine, which is the most common type of mutagenic lesion observed upon ROS formation [73]. Indeed, there was a drastic increase in oxidized guanines (Figure 21), indicating that the Pt-blue complex induced DNA damage through ROS formation in a dose dependent manner.

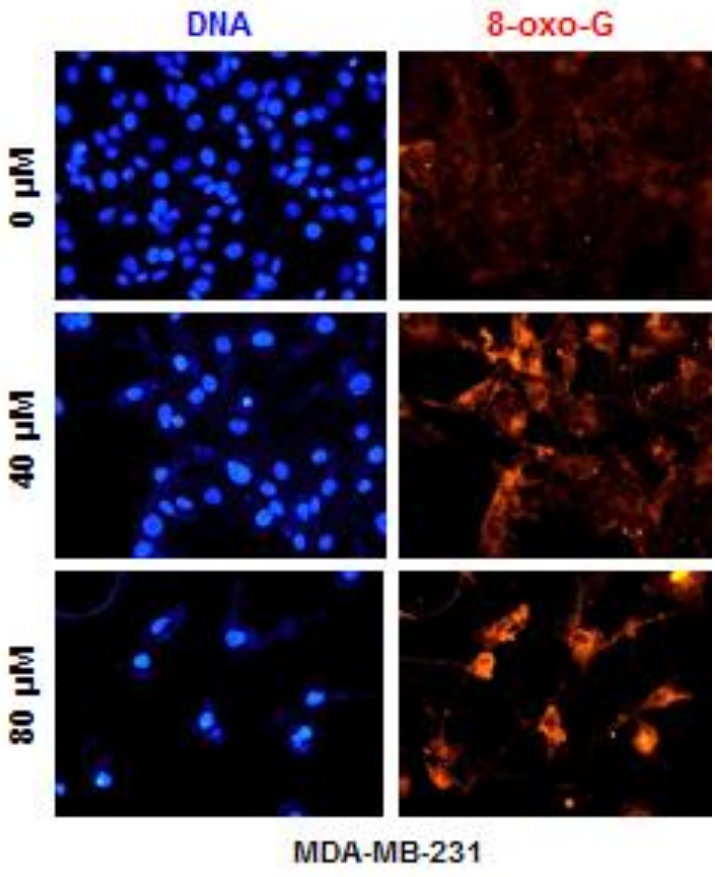

Figure 21. Cells were treated with 0, 40, or 80 µM of the Pt-blue complex and stained for 8-oxo-Guanine, a common mutagenic lesion in response to oxidative stress in cells. Cells were positive for 8-oxo-G following Pt-blue treatment indicating that the drug treatment damaged DNA possible through reactive oxygen species. DNA is visualized through DAPI staining.

In summary, our data, together with the above findings, suggested that the Pt-blue complex exerted its toxic effect through DNA damage and oxidative stress triggering the apoptotic pathways.

3.6.5. Molecular changes in response to Pt-Blue treatment

In order to understand the molecular changes in response to Pt-blue complex, a custom RT-qPCR array was designed to cover a panel of 51 genes playing a role in the regulation, induction or inhibition of apoptosis, as well as genes involved in oxidative stress response (Figure 22). The array was run in duplicate and genes that showed significant 1.5 - 2 fold up/downregulation were retested using three different extracts in duplicate. The arithmetic average of two housekeeping genes (YWHAZ and GAPDH) was used for normalization, and the gene stability number (ratio of YWHAZ to GAPDH) was close to 1 (1 ± 0.02) as expected from stable internal control genes [74]. Our analysis revealed that 6 out of 51 genes (Bag3, Bak, Bik, Bmf, Hrk and SOD) were upregulated in a consistent manner in all three biological repeats although the fold change varied between experiments. Expression of genes that were not consistent between experimental repeats (e.g. Noxa, DR4) was omitted from our analysis. Interestingly, 5 of these proteins are associated with Bcl-2, suggesting that the inactivation of Bcl-2 is one of the main events during Pt-blue induced apoptosis. Furthermore, all code for pro-apoptotic molecules (except for Bag3, which appears to have multiple functions [75]) indicating that the mechanism of action involves activation of apoptosis, rather than suppression of viability cues. Consistently, the levels of cell survival genes, Akt 1 and 2, were not significantly altered. Furthermore, intrinsic pathways of apoptosis appear to be mainly involved, since there was no significant change in the expression of death receptors (extrinsic pathway). SOD levels were also increased indicating an increase in superoxide radicals, confirming elevated ROS formation observed by our in vitro plasmid analysis and cell culture studies. Hence, our results are in accordance with our previous findings suggesting formation of oxidative stress and apoptosis as the mode of cell death in response to Pt-blue treatment.

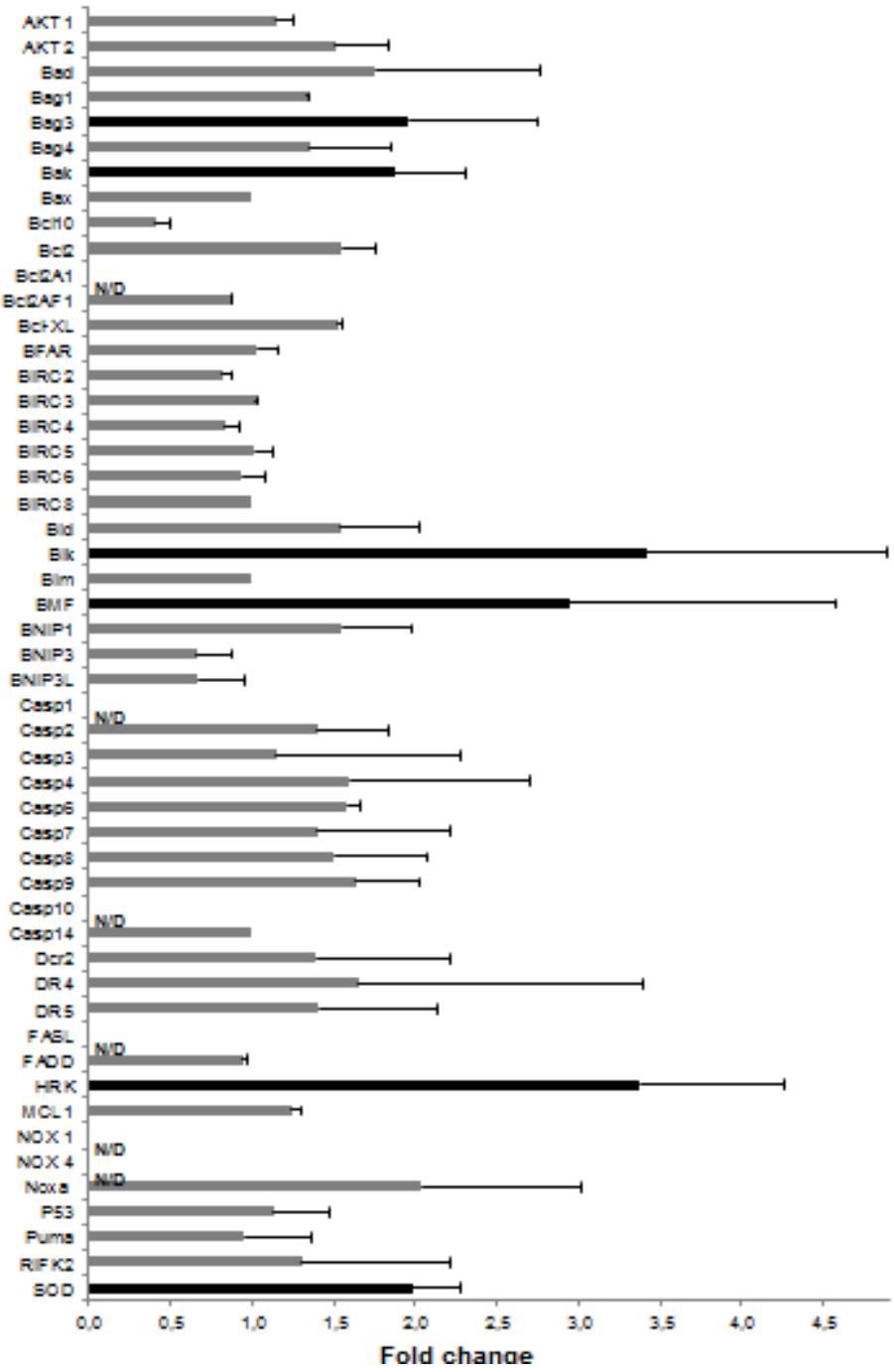

Figure 22. RT-qPCR results for 51 genes that were tested in our analysis. Gene names are given on the left of the graft. x-axis shows the expression fold change normalized to the arithmetic average of two housekeeping genes (YWHAZ and GAPDH). Black bars highlight genes that were consistently upregulated in all three biological repeats. N/D indicates genes that could not be detected.

CHAPTER 4

CONCLUSION

Four different experimental procedure was performed by using cisplatin as a starting platinum source to synthesize possible novel platinum blue complexes containing both 2-atp and NH_3 ligands. However, comparative electronic absorption spectrum studies with that of $[Pt_4(2\text{-atp})_8(H_2O)(OH)]$ surprisingly indicated the formation of the identical complex in each trial.

Electronic absorption spectroscopy is used to demonstrate the interaction of platinum blue with ct-DNA. The intensity of the characterstic band at 555 nm increased obviously with an insignificant shift after the addition of the increased amount of ct-DNA. The observed hyperchromic effect may indicate an electrostatic interaction between the complex cation and the negatively charged phosphate groups in the double helix of ct-DNA. Binding constant of the platinum blue complex is calculated as $1x10^5$ M^{-1}. UV titration experiments which were carried out at different temperature were used to determine thermodynamic data. Negative enthalpy (-61.80 kJ/mol) and entropy (−101,40 J/mol K) changes indicate van der Waals interactions and hydrogen bonding as a binding mode of a drug to DNA and hence confirm an electrostatic interaction of the positively charged complex and DNA is followed by an intercalative binding an intercalative mode of action.

Thermal decomposition of DNA double helix structure in the presence and the absence of the complex confirm the electrostatic/intercalative binding mode of the Pt-Blue complex.

The observed low in the slope of the relative viscosity of the Pt-blue-DNA adduct compared to that of DNA-EB can be associated with the lower binding constant of the platinum complex.

The addition of the complex to EB substituted DNA cause a substantial decrease in emission intensity with a red shift, suggesting that the complex bind to DNA intercalatively and exchanges with EB with a Stern-Volmer quenching constant, K_{sq}, of 0.14.

The cytotoxicity the Pt-blue complex is evaluated in different tumor cell lines indicates that the cancer cells were more sensitive to the Pt-blue complex and this compound appeared to be potential anticancer drug. The morphological assessments and tunnelling experiments strongly indicated apoptosis as the primary form of cell death.

As a conclusion, our data suggested that the Pt-blue complex exerted its toxic effect through DNA damage and oxidative stress triggering the apoptotic pathways.

REFERENCES

[1] F. A. Cotton; Wilkinson, *G.*; Murillo C. A.; Bochmann, M. (1999), Advanced Inorganic Chemistry (6th ed.), New York: Wiley-Interscience.

[2] F. A. Cotton; Geoffrey W.; Carlos A. M. (1999). Advanced Inorganic Chemistry , 1355.

[3] D. Mc Donald D., L.B. Hunt, "History of Platinum and Its allied Metals, Inc. Johnson Matthey, London, 1982.

[4] S. Reineke ,F.Lindner , G. Schwartz ,N. Seidler , K. walzer , B.Lussem and K. Leo , Nature , (2009) ,459, 234.

[5] Y. Sun, N.C. Giebink , H. Kannol , B. Ma , E. Thompson and S.R. Forrest , Nature (2006) 440, 908.

[6] A. Poloek , C. Wen Lin ,C. Ti Chen, C. Tsen Chen , J. Mater. Chem. C, (2014) 2, 10343-10356.

[7] J. A.G. Williams, J. Mater. Chem., (2014) 2 , 1791.

[8] A. Poloek , C. Wen Lin ,C. Ti Chen, C. Tsen Chen , C. Wang ,Y. Ting Chang , J. Mater. Chem. C, (2015) 3, 11163-11177.

[9] M. Kato , Bull. Chem. Soc. Jpn, 80 (2) , 287 (2007)

[10] M. D. Santana , R. Garcia- Bueno , G. Garcia , G.Sanchez , J. Garcia , J. Penes ,L. Garcia and J.L. Serrano , Dalton Trans .40(14) , 3537 (2011).

[11] E.A. Katlenok , K.P. Balashev , Optics and Spectroscopy 116 (2014) 100-104.

[12] E.A. Katlenok , K.P. Balashev , Optics and Spectroscopy 117 (2014) 3, 374-380.

[13] E.A. Katlenok, A.A. Zolotarev, K.P. Balashev, 84 (2014), 8,1593-1598.

[14] Rosenberg, B., L. Vancamp, and T. Krigas, Nature, 1965. 205: p. 698-9.

[15] B. Lippert (Ed.) , cisplatin , New York , (1999).

[16] K. Cui, L. Wang, H. Zhu, S. Gou, Y .Liu, Bioorganic & Medicinal Chemistry Letter 16 (2006) 2937-2942.

[17] D.Talancon, C. Lopez, M. Font- Bardia, T. Calvet ,J. Quirante, C. Calvis, R. Messeguer,
R. Cortes, M. Cascante, L. Baldoma , J. Badia, Journal of Inorganic Biochemistry 118 (2013) 1-12.

[18] N. Shahabadi, L. Heidari, Molecular and Biomolecular Spectroscopy 128 (2014) 377-385.

[19] S.Cerri, V. M. Piccolini, G. Santia, M.G. Bottne, S.A. De Pascali , D. Migoni , P. Iadarola , F. P. Fannizzi ,G. Bernocchi, Neurotoxicity and Teratology 33 (2011) 273-281.

[20] C.B.Du Puch , E. Barbier , A. Kraut , Y. Coute , J. Fuchs , A. Buhot , T. Livache , M. Seve , A. Favier , T. Douki , D. Gasparutto , S. Sauvaigo , J. Breton , Archives of Biochemistry and Biophysics 507 (2011) 296-303.

[21] M. Galanski ,C. Baumgartner , K. Meelich , V. B. Arion , M. Fremuth , M.A. Jakupec , P. Schluga, C. G.Hartinger, N.G v. Keyserlingk , B.K. Keppler , Inorganic Chimica Acta 357 (2004) 3237-3244.

[22] J. Kasparkova , O. Vrana , N. Farrell ,V. Brabec , Inorganic Biochem. 98 (2004) 1560-1569.

[23] H.S. Oberoi, N.V. Nukolova , A.V. Kabanov , T.K. Bronich , Advanced Drug Reviews, 65 (2013) 1667-1685.

[24] P.J. O'Dwyer , J.P. Stevenson , S.W. Johnson, Drugs 59 (suppl.4) (2000) 19.

[25] L.R.Kelland, Drugs, 59 (suppl.4) (2000) 1.

[26] A.H.Calvert, S.J. Harland, D.R. Newell, Z.H. Siddik, A.C. Jones, T.J. McElwain, S. Raju, E. Wiltshaw, I.E.Smith, J.M. Baker, M.J. Pechham, K.R. Harrap, Cancer Chemother. Pharmacol. 9 (1982) 140-147.

[27] B.Stordal, N.Pavlakis, R. Davey, Oxaliplatin for the treatment of cisplatin-resistant cancer: a systematic review, Cancer Treat .Rev.33 (2007) 347-357.

[28] A.A. Shabana ,I.S. Butler , D.F.R. Gilson , B.J. Jean-Claude, Z. S. Mouhri , M.M. Mostafa, S.I. Mostafa , Inorganic Chimica Acta 423 (2014) 242-255.

[29] A.Y.Oral, B. Cevatemer, M. Sarimahmut, C. Icsel ,V.T. Yilmaz, E. Ulukaya, Bioorg. Med. Chem. 23 (2015) 4303-4320.

[30] M. Fabijanska, k. Studzian, L. Szmigiero, A.J. Rybarczyk-Pirek, A. Pfitzner, B. Cebula-Obrzut, P. Smolewski, E. Zynera, J. Ochocki, Dalton Trans. 44 (2015) 938-947.

[31] M. Fanelli , M. Formica ,V. Fusi , L. Giorgi , M. Micheloni, Coordination Chemistry Reviews 310 (2016) 41-79.

[32] C. Perez , C. V. Diaz-Garcia , A. Agudo-Lopez , V. del Solar , S. Cabrera , M. T. Agullo-Ortuno , C. Ranninger , J. Aleman , J. A. Lopez-Martin , European Journal of Medicinal Chemistry 76 (2014) 360-368.

[33] M.A. Carvalho , S. M. Shishido , B. C. Souza , R. de Paiva , A. F. Gomes , F. C. Gozzo , A. Formiga , P. P. Corbi ,Molecular and Biomolecular Spectroscopy 122 (2014) 209-215.

[34] S.R. Bhowmik , S. Gangopadhyay, P. K. Gangopadhyay , Journal of Coordination Chemistry 58 (2005), 795-801.

[35] J.K. Barton, H.N. Rabinowitz, D.J.Szalda, S.J. Lippard. J. Am. Chem. Soc., 99, 2827(1977).

[36] M.P. Laurent , J. Bisco, H.H. Patterson , J. Am. Chem. Soc., 102, 6576 (1980).

[37] J.P. Davidson, P.J. Faber, R.G. Fisher, Cancer Chemother. Rep., (1975) ,59, 287.

[38] İ. Erilhan, Master of Science Thesis in Chemistry, Middle East Technical University, Ankara, Turkey, (2007).

[39] Khan, N.U., et al., Eur. J. Med. Chem.,(2011). 46(10): p. 5074-85.

[40] Abassi, P., et al., J. Photochem. Photobiol. B., (2013). 122: p. 61-7.

[41] Reddy, P.R. and A. Shilpa, Polyhedron, (2011). 30: p. 565-72.

[42] Sasmal, P.K., A.K. Patra, and A.R. Chakravarty, J. Inorg. Biochem.,(2008). 102(7): p. 1463-72.

[43] Zhang, G., et al., Journal of Molecular Structure, (2009). 923(1-3): p. 114-19.

[44] Korkmaz, F., D. Altunoz Erdogan, and Ş. Özalp Yaman, New J. Chem., (2015). 39: p. 5676-85.

[45] Kalaivani, P., et al., Metallomics, (2012). 4(1): p. 101-13.

[46] Waring, M.J., J. Mol. Biol.,(1965). 13(1): p. 269-82.

[47] Baba, Y., et al., (1982) , American Chemical Society: Washington DC, USA.

[48] B.N. Rajesh, S.T. Emily, L.K. Shalawn, J.M. Catherine, Inorg. Chem., 37 (1988) 85.

[49] Pulimamidi, R. Nomula, R. Pallepogu, H. Shaik, Eur. J. Med. Chem, 79 (2014) 117-27.

[50] S. Arounagiri, B.G. Maiya, Inorg. Chem., 35 (14) (1996) p. 4267-70.

[51] Nair , R.B., et al., Inorganic Chemistry, (1998). 37(1): p. 139-41.

[52] Eriksson, M., et al., Journal of American Chemical Society, (1992). 114(12): p. 4933-34.

[53] Silvestri, A., et al., J. Inorg. Biochem., (2007). 101(5): p. 841-8.

[54] Shahabadi, N. and A. Fatahi, Journal of Molecular Structure, (2010). 970(1-3): p. 90-5.

[55] Satyanarayana, S., J.C. Dabrowiak, and J.B. Chaires, Biochemistry, (1993). 32(10): p. 2573-84.

[56] Shahabadi, N., et al., Bioinorg. Chem. App.l, 2011. (2011): p. 525794.

[57] Mudasir, N. Yoshioka, and H. Inoue, J. Inorg. Biochem, (1999). 77(3-4): p. 239-47.

[58] Reddy, P.R., K.S. Rao, and B. Satyanarayana, Tetrahedron Letters, (2006). 47(41): p. 7311-15.

[59] Maheswari, P.U. and M. Palaniandavar, Inorganica Chimica Acta, (2004). 357(4): p. 901-12.

[60] Chauhan, M. and F. Arjmand, Chemistry and Biodiversity, (2006). 3(6): p. 660-76.

[61] Kelly, J.M., et al., Nucleic. Acids Res., (1985). 13(17): p. 6017-34.

[62] Chen, L.M., et al., J. Inorg. Biochem, (2008). 102(2): p. 330-41.

[63] López, B.R. and L.B. Loeb, Tetrahedron Letters, (1996). 37(31): p. 5437–40.

[64] Sasmal, P.K., et al., Inorganic Chemistry, (2009). 49(3): p. 849–859

[65] Raman, N. and N. Pravin, Eur. J. Med. Chem, (2014). 80: p. 57-70.

[66] Li, F.H., et al., J. Inorg. Biochem.,(2006). 100(1): p. 36-43.

[67] Acilan, C., et al., Smooth muscle cells isolated from thoracic aortic aneurysms exhibit increased genomic damage, but similar tendency for apoptosis. DNA Cell

Biol, 2012. 31(10): p. 1523-34.

[68] Adiguzel, Z., et al., Biochemical and proteomic analysis of a potential anticancer agent: Palladium(II) Saccharinate complex of terpyridine acting through double strand break formation. J Proteome Res, 2014. 13(11): p. 5240-9.

[69] Adiguzel, Z., et al., Evaluation of apoptotic molecular pathways for smooth muscle cells isolated from thoracic aortic aneurysms in response to oxidized sterols. Mol Biol Rep, 2014. 41(12): p. 7875-84.

[70] Hoper, J., Spectrophotometric in vivo determination of local mitochondrial metabolism by use of a tetrazolium salt. Physiol Meas, 1997. 18(1): p. 61-6.

[71] Valdiglesias, V., et al., gammaH2AX as a marker of DNA double strand breaks and genomic instability in human population studies. Mutat Res, 2013. 753(1): p. 24-40.

[72] Senkal, M., et al., Mitoxantrone-induced DNA strand breaks in cell-cultures of malignant human astrocytoma and glioblastoma tumors. J Neurooncol, 1997. 32(3): p. 203-8.

[73] Fortini, P., et al., 8-Oxoguanine DNA damage: at the crossroad of alternative repair pathways. Mutat Res, 2003. 531(1-2): p. 127-39.

[74] Vandesompele, J., et al., Accurate normalization of real-time quantitative RT-PCR data by geometric averaging of multiple internal control genes. Genome Biol, 2002. 3(7): p. Research0034.

[75] Rosati, A., et al., BAG3: a multifaceted protein that regulates major cell pathways. Cell Death Dis, 2011. 2: p. e141.